



Wild-type sTREM2 blocks A β aggregation and neurotoxicity, but the Alzheimer's R47H mutant increases A β aggregation

Received for publication, February 5, 2021, and in revised form, March 26, 2021 Published, Papers in Press, April 3, 2021, <https://doi.org/10.1016/j.jbc.2021.100631>

Anna Vilalta^{1,‡}, Ye Zhou^{2,‡}, Jean Sevalle^{2,‡}, Jennifer K. Griffin^{2,‡}, Kanayo Satoh^{2,‡}, David H. Allendorf¹, Suman De³, Mar Puigdemívol¹, Arturas Bruzas¹, Miguel A. Burguillos^{1,4}, Roger B. Dodd^{3,4}, Fusheng Chen², Yalun Zhang², Patrick Flagmeier⁵, Lisa-Maria Needham⁵, Masahiro Enomoto⁶, Seema Qamar⁴, James Henderson⁴, Jochen Walter⁷, Paul E. Fraser², David Klenerman^{5,8}, Steven F. Lee⁵, Peter St George-Hyslop^{2,4,*}, and Guy C. Brown^{1,*}

From the ¹Department of Biochemistry, University of Cambridge, Cambridge, United Kingdom; ²Departments of Medicine (Neurology) and Medical Biophysics, University of Toronto and University Health Network, Toronto, Ontario, Canada; ³AstraZeneca, Cambridge, United Kingdom; ⁴Cambridge Institute for Medical Research, Cambridge, United Kingdom; ⁵Department of Chemistry, University of Cambridge, Cambridge, United Kingdom; ⁶Princess Margaret Cancer Centre, University Health Network, Department of Medical Biophysics, University of Toronto, Toronto, Ontario, Canada; ⁷Molecular Cell Biology, Department of Neurology, University of Bonn, Bonn, Germany; and ⁸Cambridge Dementia Research Institute, Cambridge Biomedical Campus, Cambridge, United Kingdom

Edited by Peter Cresswell

TREM2 is a pattern recognition receptor, expressed on microglia and myeloid cells, detecting lipids and A β and inducing an innate immune response. Missense mutations (e.g., R47H) of TREM2 increase risk of Alzheimer's disease (AD). The soluble ectodomain of wild-type TREM2 (sTREM2) has been shown to protect against AD *in vivo*, but the underlying mechanisms are unclear. We show that A β oligomers bind to cellular TREM2, inducing shedding of the sTREM2 domain. Wild-type sTREM2 bound to A β oligomers (measured by single-molecule imaging, dot blots, and Bio-Layer Interferometry) inhibited A β oligomerization and disaggregated preformed A β oligomers and protofibrils (measured by transmission electron microscopy, dot blots, and size-exclusion chromatography). Wild-type sTREM2 also inhibited A β fibrillization (measured by imaging and thioflavin T fluorescence) and blocked A β -induced neurotoxicity (measured by permeabilization of artificial membranes and by loss of neurons in primary neuronal–glial cocultures). In contrast, the R47H AD-risk variant of sTREM2 is less able to bind and disaggregate oligomeric A β but rather promotes A β protofibril formation and neurotoxicity. Thus, in addition to inducing an immune response, wild-type TREM2 may protect against amyloid pathology by the A β -induced release of sTREM2, which blocks A β aggregation and neurotoxicity. In contrast, R47H sTREM2 promotes A β aggregation into protofibril that may be toxic to neurons. These findings may explain how wild-type sTREM2 apparently protects against AD *in vivo* and why a single copy of the R47H variant gene is associated with increased AD risk.

A prominent neuropathological feature of Alzheimer's disease (AD) is the presence of extracellular deposits of the

amyloid β -peptide in amyloid plaques, surrounded by activated microglia (1–3). The importance of this microglial response to the pathogenesis of AD has been highlighted by the recent discovery of sequence variants in multiple genes expressed in microglia that alter risk for AD. Prominent among these microglial AD-risk genes is the “triggering receptor expressed on myeloid cells 2” (TREM2) (4–6), of which there are several missense mutations in the ectodomain, including R47H, associated with increased risk for AD (4–6). The biological mechanisms underlying this association remain unclear.

Full-length TREM2 is expressed on the plasma membrane of microglia, where it can be cleaved by one or more metalloproteases to produce (i) a membrane-bound C-terminal fragment (CTF); and (ii) an N-terminal fragment consisting of the soluble ectodomain of TREM2 (sTREM2), which is released into the extracellular space (7–9). sTREM2 has been thought of as a nonfunctional, degradation product of TREM2 and used as a biomarker of microglial activation (10–12). However, several recent observations suggest the possibility that sTREM2 per se may play a role protecting against AD by interacting with A β . First, oligomeric A β binds to TREM2 and to sTREM2-Fc fusion protein (13–15), suggesting that sTREM2 might bind A β and potentially affect its aggregation state. Second, injection or expression of sTREM2 in the hippocampus of 5xFAD mice reduces both amyloid plaque load and memory deficits (16), indicating that sTREM2 inhibits amyloid pathology somehow. Third, in transgenic mouse models overproducing A β , the knockout of TREM2 expression accelerates amyloid plaque seeding (17) and the plaques have increased protofibrillar halos and hotspots (3, 16, 18), indicating that either TREM2 or sTREM2 inhibits plaque formation. Fourth, in the earliest presymptomatic stages of AD, at the time of A β deposition, sTREM2 levels in cerebrospinal fluid (CSF) are lower than in healthy controls (10, 19), consistent with sTREM2 being an endogenous inhibitor of A β

[‡] These authors contributed equally to this work.

* For correspondence: Peter St George-Hyslop, phs22@cam.ac.uk; Guy C. Brown, gcb3@cam.ac.uk.

sTREM2 blocks A β aggregation and neurotoxicity

deposition. However, the CSF A β levels rise in the early symptomatic stages of AD and then decline again at later stages of AD (11, 12). Fifth, mild cognitive impairment (MCI) and AD patients with higher sTREM2 levels in CSF have slower brain atrophy, cognitive decline, and clinical decline (20, 21), consistent with sTREM2 inhibiting AD progression. Sixth, healthy controls and MCI patients with higher sTREM2 levels in CSF have slower progression of amyloid and tau deposition (22), consistent with sTREM2 inhibiting A β aggregation and subsequent tau pathology.

All of these *in vivo* findings are compatible with the hypothesis that sTREM2 might protect against AD, potentially by impacting A β aggregation. To explore this hypothesis and the mechanisms involved, we investigated the interaction of A β with sTREM2 *in vitro*. We report that soluble A β oligomers bind TREM2 receptor on microglia and induce shedding of sTREM2. Next, we show that sTREM2 can bind and disaggregate A β oligomers, block A β fibrillization, and reduce A β neurotoxicity. These activities are attenuated in the R47H TREM2 holoprotein and R47H sTREM2. Moreover, the R47H sTREM2 promotes formation of morphologically distinct A β protofibrils. These data indicate additional mechanisms by which TREM2 protects against Alzheimer's disease and a previously unrecognized mechanism by which the R47H mutant increases risk.

Results

A β oligomers bind TREM2 holoprotein and induce TREM2 ectodomain shedding

To confirm that TREM2 can act as a cell surface receptor for A β oligomers, we treated mouse primary microglia or TREM2-transfected HeLa cells with A β 42 oligomers that have been characterized both by electron microscopy and by oligomer/fibril specific antibodies (Fig. S1; note only A β 42 was used in this work and will be referred to as A β henceforth). We then immunoprecipitated TREM2 from lysates of these cells and found that A β co-immunoprecipitated with endogenous TREM2 on primary microglia from wild-type mice, but not on microglia from TREM2^{-/-} knockout mice (Fig. S2i). The A β binding was prevented by TREM2-blocking antibody (Fig. S2ii). Oligomeric A β bound to TREM2 but not TREM1 (Fig. S2iii). Monomeric A β co-immunoprecipitated with TREM2 less efficiently than oligomeric A β (Fig. S2, *iv* and *v*, $p = 0.03$). The TREM2: A β oligomer interaction is at least partially specific because neither of two other neurodegeneration-associated oligomeric proteins (oligomeric α -synuclein or oligomeric Tau) bound to TREM2 even in HeLa cells overexpressing TREM2 and DAP12 (Fig. S3). These results confirm and extend the work of other groups showing that oligomeric A β binds TREM2 (13–15).

We next tested the consequences of A β oligomers binding to TREM2 on primary microglia. A β oligomers induced release of sTREM2 into the medium of primary microglia from wild-type mice, but not microglia from mice engineered to express R47H TREM2 (Fig. S4i, $p < 0.05$). To study this effect in more detail, we stably expressed human TREM2 (together with

human DAP12) in HEK293 cells. Treatment of these cells with A β oligomers resulted in dose-dependent release of sTREM2 into the medium and the accumulation of TREM2-CTF in cell lysates (Fig. 1, A and B & Fig. S4ii). In contrast, treatment with A β monomers or fibrils resulted in no modulation of sTREM2's release (Figs. 1C and S5). We have previously shown that this shedding event occurs rapidly, within 1 h of A β oligomer binding, but that FL-TREM2 levels remain constant due to ongoing new synthesis of FL-TREM2 (8). The release of sTREM2 induced by oligomeric A β was attenuated in HEK293 cells expressing R47H TREM2 (Fig. 1B & Figs. S4ii and S5). Thus, oligomeric A β stimulates release of sTREM2 (potentially by endoproteolysis) from cells expressing wild-type TREM2, but less so from cells expressing R47H TREM2.

Wild-type sTREM2 binds A β oligomers better than R47H TREM2

Because A β oligomers bind to TREM2 and induce shedding of sTREM2, it is of interest whether sTREM2 itself binds A β oligomers. Three groups reported that wild-type sTREM2 fused to the Fc domain of IgG binds oligomeric A β (13–15). However, Zhao *et al.* (13) and Zhong *et al.* (14) found that R47H sTREM2-Fc bound less than wild-type to A β , while Lessard *et al.* (15) found that they bound equally. We applied three orthogonal assays using an approach that did not require fusion of sTREM2 to the Fc domain of IgG, to reassess this question. Firstly, we examined this interaction at the molecular level using single-molecule total internal reflection fluorescence (TIRF) microscopy-based two-color coincidence detection (23). HiLyte 488-dye labeled A β was oligomerized and TAMRA-dye labeled sTREM2 added and imaged. Monomeric A β bleaches rapidly, so colocalization of A β and sTREM2 before and after bleaching enabled us to distinguish between monomers and oligomers. These experiments revealed that wild-type sTREM2 bound oligomeric A β much more than monomeric A β (Fig. 1, D and E) and that R47H sTREM2 bound less well to oligomeric A β than wild-type sTREM2 did (Fig. 1F). Second, this result was confirmed by a semiquantitative dot blot assay, which showed that wild-type sTREM2 preferentially bound oligomeric A β over monomeric A β and that R47H sTREM2 bound less of both forms of A β (Fig. S6, *i* and *ii*).

Third, we used Bio-Layer Interferometry (BLI) (24) to quantitatively assess the A β oligomer: sTREM2 interaction by immobilizing biotin-A β oligomers on Streptavidin biosensors and then exposing them to sTREM2. These studies suggested that sTREM2 associated with A β oligomers with two different rates and dissociated from A β oligomers with two different rates (Fig. S6, *iii* and *iv*), consistent with sTREM2 binding to different A β oligomer sizes with different affinities. Best fit association and dissociation curves for both wild-type and R47H sTREM2 were with a 2:1 heterogeneous ligand model. In agreement with the semiquantitative experiments described above, these BLI studies confirmed that R47H sTREM2 bound A β oligomers less well than wild-type sTREM2 (Table S1: TREM2 WT $K_{D1} = 2.00 \pm 0.15 \mu\text{M}$, $K_{D2} = 0.29 \pm 0.08 \mu\text{M}$; TREM2 R47H mutant $K_{D1} = 11.70 \pm 5.97 \mu\text{M}$, $K_{D2} = 1.22 \pm 0.30 \mu\text{M}$; where K_{D1} is the dissociation constant of the

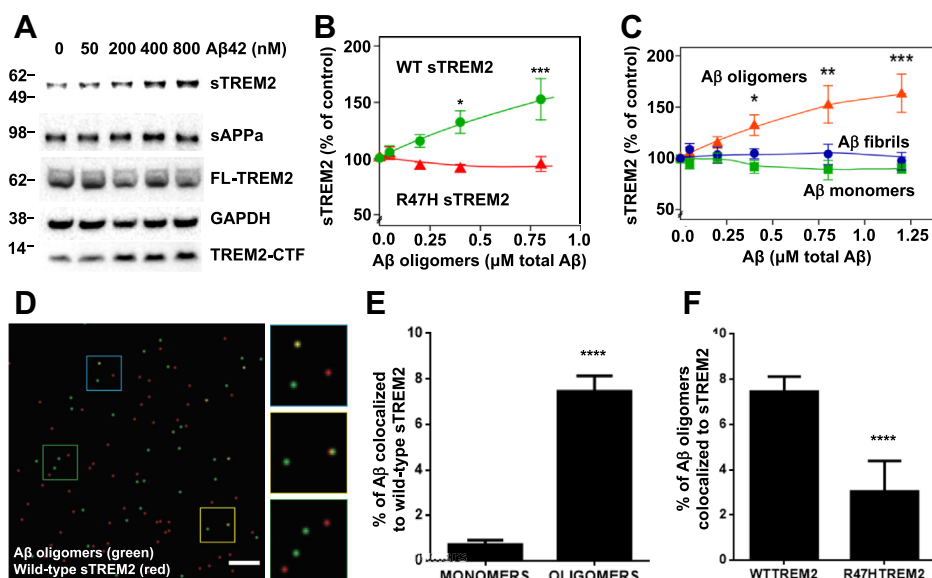


Figure 1. A β oligomers induce TREM2 proteolysis and sTREM2 release, which then binds A β oligomers, but R47H sTREM2 binds less. *A*, western blot of cell lysate and unprocessed supernatant (sTREM2) of HEK293 cells coexpressing human DAP12 and full-length N-terminally-tagged wild-type (WT) human TREM2 (FL-TREM2) 16 h after adding A β oligomers. This blot and those for A β monomers and fibrils are reproduced in [Figure S5](#) for comparison. *B*, quantification of sTREM2 release from transfected HEK293 cells expressing wild-type (green line) and R47H TREM2 (red line) (green line), monomers (green line), or fibrils (blue line). For both (*B* and *C*) error bars = SEM; * $p < 0.05$ ** $p < 0.01$ *** $p < 0.001$, $n = 3$ independent experiments; one-way ANOVA with Tukey's post-hoc multiple comparisons test. *D*, example field of single-molecule TIRF imaging of mixture of A β oligomers (green) and wild-type TREM2 ectodomain (red), where colocalized spots appear yellow. Scale bar: 1 micron. Magnified image of three sections of field at right. *E*, proportion of monomeric or oligomeric A β colocalized with wild-type sTREM2. *F*, proportion of A β oligomers colocalized with wild-type or R47H TREM2 ectodomain. For (*E* and *F*), error bars = SEM; **** $p < 0.0001$, $n = 3$ independent preparations, each analyzed in nine fields each; two-tailed *t*-test of significance.

predominant interaction within the heterogeneous population of A β species).

Wild-type sTREM2 inhibits A β oligomerization and dissolves A β oligomers, whereas R47H sTREM2 induces A β protofibrils

Because sTREM2 bound to A β oligomers, we next investigated whether sTREM2 affected A β oligomerization. We incubated 22 μ M monomeric A β \pm 0.22 or 0.44 μ M sTREM2 (wild-type or R47H) for 3 h at 37 $^{\circ}$ C, *i.e.*, conditions known to generate A β oligomers. The formation of A β oligomers was then assessed by transmission electron microscopy (TEM) ([Figs. 2](#) and [S7](#)); dot blotting with A11 antioligomer antibody; and by high-performance liquid chromatography size-exclusion chromatography (HPLC-SEC) experiments ([Fig. S8](#)). These experiments revealed that preincubation of A β monomers with wild-type sTREM2 (at molar ratios of 1:50 and 1:100 sTREM2: A β) inhibited A β oligomerization ([Fig. 2A](#)) quantified by area ([Fig. 2B](#)) or number ([Fig. S7i](#)). SEC and antibody dot blots confirmed that sTREM2 inhibited formation of A β oligomers ([Fig. S8i](#)). Analysis of the size distribution of A β oligomers by TEM revealed that wild-type sTREM2 reduced the abundance of small oligomers (oligomer size <60 nm 2) and eliminated larger oligomers (oligomer size >70 nm 2) ([Fig. S9i](#)).

In contrast, R47H sTREM2 did not block A β oligomerization, but instead promoted the formation of morphologically-distinct A β protofibrils ([Fig. 2, C and D](#); [Figs. S7ii](#) and [S9ii](#)). Thus, the presence of wild-type sTREM2 reduces the formation of A β oligomers, particularly larger oligomers, and in stark contrast, R47H sTREM2 induces A β monomers to form A β protofibrils.

To study reversal of oligomerization, preassembled A β oligomers were diluted to 2 μ M and mixed with wild-type or R47H sTREM2 (at molar ratios of sTREM2: total A β of 1:5 and 1:1) and incubated for 30 min at 37 $^{\circ}$ C. The A β assemblies were then assessed using the same methods as above. This experiment revealed that wild-type sTREM2 disaggregated preformed A β oligomers (TEM in [Fig. 2, C and D](#) and [Fig. S7ii](#); anti-A11 dot blot and HPLC-SEC assays in [Fig. S8ii](#)). Wild-type sTREM2 strongly reduced the abundance of all but the very smallest oligomers ([Fig. 2C & Fig. S9ii](#)). In contrast, R47H sTREM2 increased the abundance of A β oligomers and induced the formation of morphologically-distinct A β protofibrils ([Fig. 2C & Figs. S7ii](#) and [S9ii](#)). A β protofibrils are large, linear A β oligomers, formed from A β monomers in a variety of conditions ([25, 26](#)), and are observed in CSF of MCI and AD patients but not healthy controls ([27](#)).

We repeated these experiments at lower concentrations, using preformed A β oligomers at 100 nM A β (monomer equivalent) incubated with 20 or 100 nM sTREM2. Wild-type sTREM2 (at either concentration) induced rapid dissolution of the A β oligomers ([Figs. S10](#) and [S11](#)). In contrast, treatment with R47H sTREM2 induced aggregation of A β oligomers into much larger A β assemblies ([Figs. S10](#) and [S11](#)).

Wild-type sTREM2 inhibited and reversed A β fibrillization, whereas R47H was less effective

Because wild-type sTREM2 inhibited A β oligomerization and disaggregated A β oligomers, we decided to test whether sTREM2 affected A β fibrillization. In the absence of sTREM2,

sTREM2 blocks A β aggregation and neurotoxicity

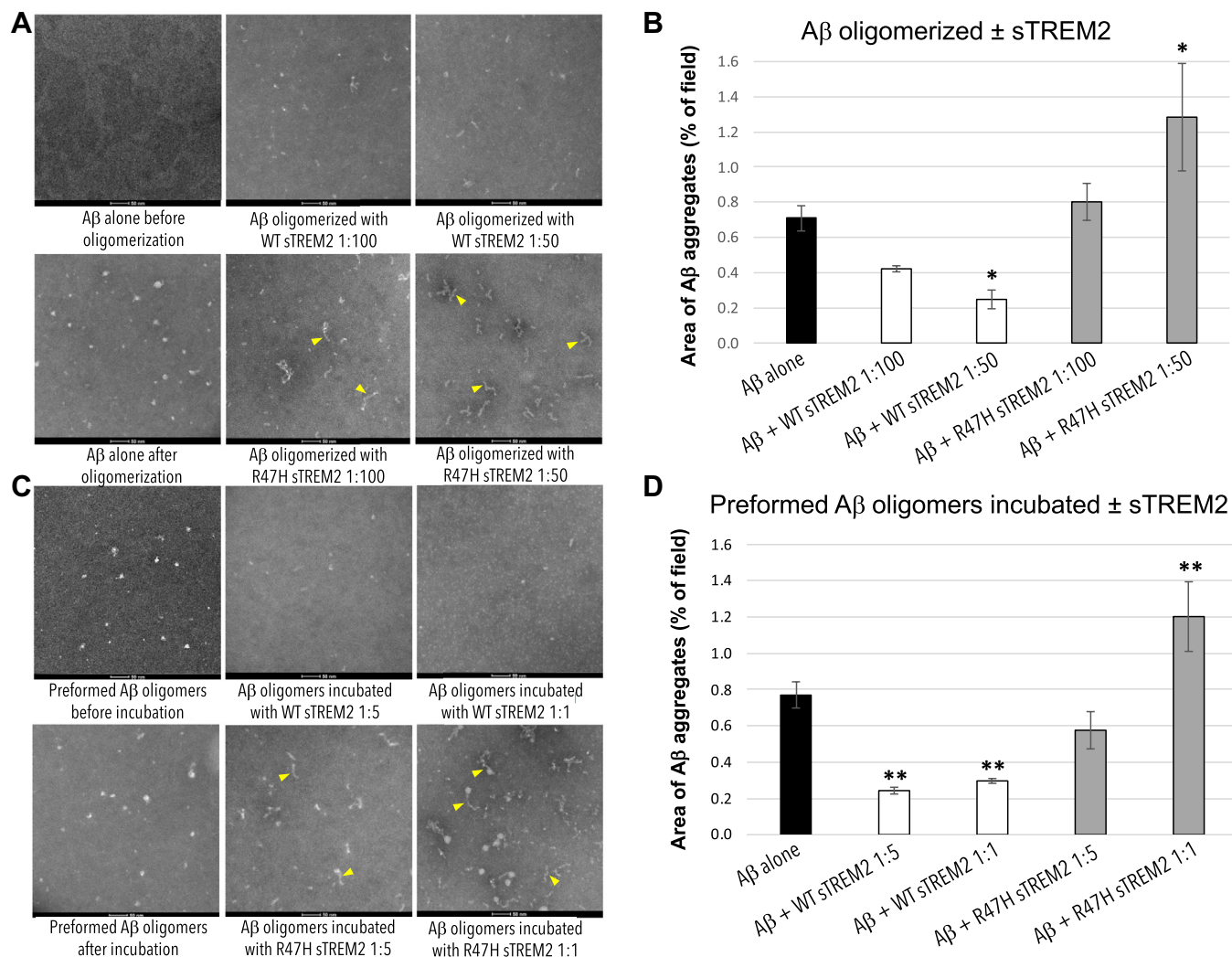


Figure 2. Wild-type sTREM2 inhibits A β oligomerization and disaggregates A β oligomers, whereas R47H sTREM2 converts A β to protofibrils. *A*, A β was aggregated for 3 h at 37 °C \pm WT sTREM2 or R47H at molar ratios of 1:100 or 1:50 (sTREM2: A β). TEM images revealed that WT sTREM2 reduced A β oligomerization, whereas R47H sTREM2 increased protofibrils (indicated by yellow arrowheads) and amorphous oligomers. *B*, quantification of three experiments indicated that WT sTREM2 decreased and R47H increased area of A β aggregates. *C*, preformed A β oligomers were treated with WT sTREM2 or R47H at molar ratios of 1:5 or 1:1 for 30 min. TEM images revealed that preformed A β oligomers were disaggregated by WT sTREM2 but formed more globular A β oligomers and protofibrils with R47H sTREM2. *D*, quantification confirmed decreased area of A β aggregates with WT sTREM2 and increased area with R47H sTREM2. For both (*B* and *D*), error bars represent SD, and statistical analysis was performed using one-way ANOVA followed by Bonferroni's multiple comparison test ($n = 3$ for each, * $p < 0.05$ versus A β oligomer, ** $p < 0.01$ versus preformed A β oligomers).

A β (10 μ M) fibrillized with standard lag-phase kinetics as measured with Thioflavin T fluorescence. However, 1 μ M of wild-type sTREM2 almost completely prevented A β fibrillization (Fig. 3, A–C). In total, 1 μ M of R47H sTREM2 did not prevent A β fibrillization, but the Thioflavin T fluorescence was lower (Fig. 3A), suggesting fibrils with less β sheet structure. Repeating these experiments, at lower concentrations and higher temperature, gave similar results. Thus, fibrillization of 2 μ M A β was substantially delayed by 20 nM sTREM2 (*i.e.*, a 100:1 ratio) and prevented by 1 μ M sTREM2 (Fig. 3D). In contrast, at the same low dose (20 nM), R47H sTREM2 had minimal effect on A β fibrillization (Fig. 3E).

To test whether sTREM2 could disaggregate fibrils of A β , small fibrils were preassembled and diluted to 2 μ M (monomer equivalent) and mixed with wild-type or R47H sTREM2 (at molar ratios of sTREM2: total A β of 1:1) and incubated for

30 min, 2 h, or 24 h at 37 °C. Wild-type sTREM2 induced rapid and complete disaggregation of the preformed A β fibrils, whereas R47H sTREM2 had little effect on fibrils (Fig. 3, G–I; Fig. S12), although there may be an increase in oligomers (Fig. 3H).

Wild-type sTREM2 inhibits A β -induced membrane permeabilization and neurotoxicity, while R47H sTREM2 increases A β -induced neurotoxicity

Because sTREM2 bound A β oligomers and inhibited A β oligomerisation and fibrillization, we next tested whether sTREM2 affected the neurotoxicity of A β . A β neurotoxicity is thought to be mediated by two different mechanisms—namely by permeabilization of neuronal membranes (28) and by microglial activation (28, 29).

Consequently, we initially used nanosized phospholipid membrane vesicles containing a calcium-sensitive fluorophore

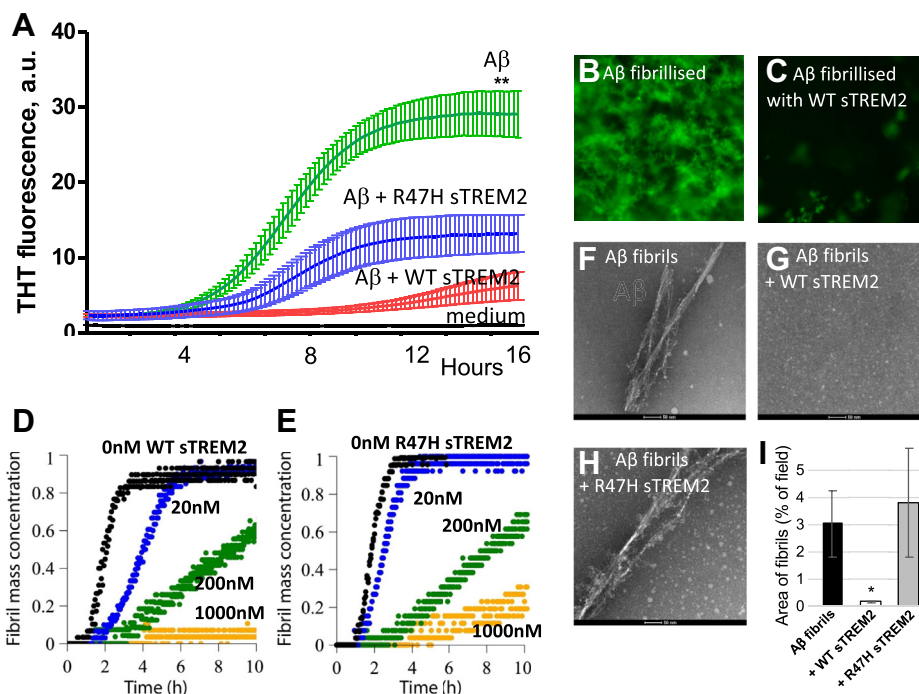


Figure 3. Wild-type sTREM2 blocks A β fibrillation, but R47H inhibits less. *A*, 10 μ M of monomeric A β was incubated at 30°C in DMEM/F12 with 10 μ M thioflavin T (THT) \pm 1 μ M wild-type or R47H sTREM2, and the fluorescence followed over time. Means and SD of three separate experiments are shown. There was significant difference ($p < 0.01$, **) between the final fluorescence of the A β v A β + WT sTREM2 samples. At the end of the assay, (*B*) in the absence of sTREM2, and (*C*) presence of wild-type sTREM2, the bottom of the well was imaged using a fluorescence microscope with a $\times 40$ objective. *D*, 2 μ M of monomeric A β was incubated at 37°C in phosphate buffer with 10 μ M THT +0, 0.02, 0.2, or 1.0 μ M wild-type sTREM2, and the fluorescence followed over time. *E*, 2 μ M of monomeric A β was incubated at 37°C in phosphate buffer with 10 μ M THT +0, 0.02, 0.2, or 1.0 μ M R47H sTREM2, and the fluorescence followed over time. Preformed A β fibrils were either (*F*) untreated, (*G*) treated with WT sTREM2, or (*H*) treated with R47H sTREM2 at molar ratios of 1:1 and TEM imaged after 2 h. *I*, quantification of the area of A β fibrils confirmed that WT sTREM2 decreased A β fibrils, and R47H sTREM2 had no effect. Images (*F*–*H*) and data (*I*) are reproduced in Figure S12 with those for 30 min and 24 h for comparison. Error bars represent SD. Statistical analysis was performed using one-way ANOVA followed by Bonferroni's multiple comparison test ($n = 3$ –8, * $p < 0.05$ versus preformed A β fibril).

to explore the ability of A β to permeabilize membranes. Prior work has shown that A β oligomers (but not monomers or fibrils) can permeabilize these membranes (28). We found that wild-type sTREM2 and R47H sTREM2 proteins themselves had no effect on membrane permeabilization when added in the absence of A β (Fig. S13*i*). By contrast, A β oligomerized for 6 h in the absence of sTREM2 induced permeabilization of the vesicles. However, A β oligomerized in the presence of wild-type sTREM2 (at molar ratios of sTREM2: total A β of 1:10) induced significantly less permeabilization (Fig. 4*A*). Wild-type sTREM2 also inhibited the permeabilization induced by preformed A β oligomers (at a 1:1 M ratio) (Fig. 4*B*). The simplest explanation for this inhibition of permeabilization is our previous finding that wild-type sTREM2 inhibits A β oligomerization and disaggregates A β oligomers at these concentrations. However, the binding of wild-type sTREM2 to A β oligomers might also reduce their toxicity.

When these experiments were repeated using R47H sTREM2 (at a molar ratio of sTREM2: total A β of 1:10), we found that A β oligomers formed in the presence of R47H sTREM2 also induced less permeabilization than A β oligomerized alone but allowed more permeabilization than A β oligomerized with wild-type sTREM2 (Fig. 4*A*). In contrast to wild-type sTREM2, R47H sTREM2 did not significantly inhibit permeabilization induced by preformed A β oligomers (Fig. 4*B*). These results are consistent with wild-type sTREM2

reducing A β oligomer abundance but R47H sTREM2 not reducing A β oligomer abundance (Fig. 2).

We next tested whether sTREM2 could block the neurotoxicity induced by A β in neuronal–glial cocultures. We have previously shown that 250 nM A β induces slow, progressive neuronal loss mediated by microglia in this coculture system (29). We found that 250 nM A β induced neuronal loss over 3 days, and this A β -induced neuronal loss was substantially reduced by cotreatment with 25 nM wild-type sTREM2 (Fig. 4, *C* and *D*). In contrast, cotreatment of the cultures with 25 nM R47H sTREM2 increased the neuronal loss above the level induced by 250 nM A β alone (Fig. 4*D*). Microglial density was not affected by the treatments; and wild-type and R47H sTREM2 proteins by themselves had no significant effect on neuronal loss (Fig. S13*ii*). As membrane permeabilization is thought to be mediated by smaller A β oligomers, while microglial activation is thought to be mediated by larger A β aggregates (28), our finding that R47H sTREM2 increased A β -induced neuronal loss (Fig. 3*D*), which is known to be microglia-mediated (29), is consistent with R47H sTREM2 increasing larger A β aggregates (Fig. 2). However, we can't rule out sTREM2 acting directly on the microglia (16) to modify neurotoxicity. Wild-type sTREM2 may also be protecting by simply binding A β oligomers, preventing their neurotoxicity, but at the molar ratios, concentrations, and measured affinities of sTREM2 and A β oligomers, the proportion of A β oligomers

sTREM2 blocks A β aggregation and neurotoxicity

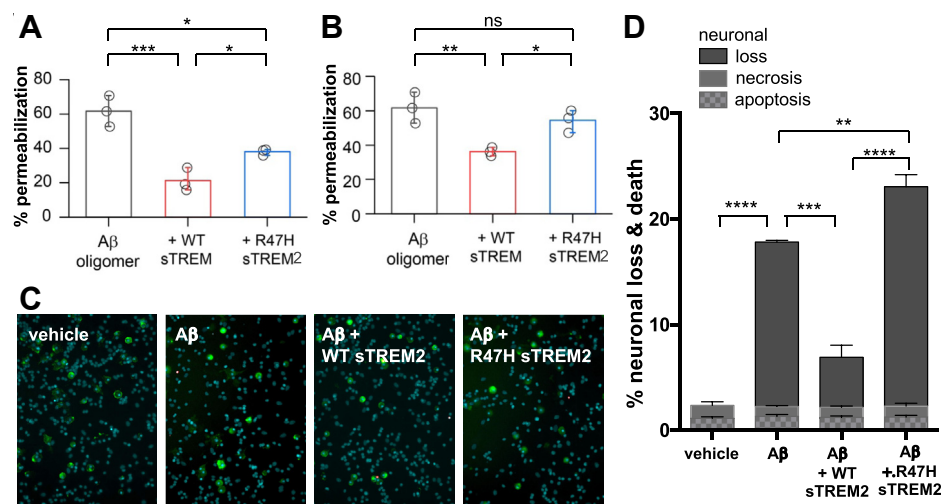


Figure 4. Wild-type sTREM2 blocks A β -induced membrane permeabilization and neuronal loss, but R47H sTREM2 inhibits less. **A**, 10 μ M of monomeric A β was aggregated \pm 1 μ M wild-type (WT) or R47H human sTREM2 for 6 h, diluted to 200 nM, and membrane permeabilization assay was performed. Error bars = SD of three independent experiments; ** p < 0.01; statistics: two-sample t -test. **B**, 10 μ M of monomeric A β was aggregated for 6 h, diluted to 200 nM, then incubated for 30 min with vehicle, 200 nM WT sTREM2 or R47H sTREM2, before the membrane permeabilization assay was performed. Error bars = SD of three independent experiments; ** p < 0.01; statistics: two-sample t -test. **C** and **D**, mixed neuronal–glial cocultures were treated with either: vehicle, 250 nM monomeric A β , 250 nM A β + 25 nM WT sTREM2 or 250 nM A β + 25 nM R47H sTREM2. Three days later, cultures were stained with isolectin B4 (green, to identify microglia), propidium iodide (red, to identify dead cells), and Hoechst 33342 (blue, to identify cells and whether apoptotic) and imaged (representative fields: **C**), and the number of apoptotic, necrotic, and healthy neurons were quantified (mean data: **D**). Loss is the decrease in neuronal density relative to vehicle-treated cultures. Error bars = SEM; ** p < 0.01, *** p < 0.001, **** p < 0.0001; n = 4 independent experiments on separate cell cultures. Statistical analysis was by one-way ANOVA and Tukey’s post-hoc test.

bound to sTREM2 is likely to be small in the conditions used, so the contribution of this mechanism to neuroprotection is likely to be small. However, in order to distinguish between these mechanisms more clearly, we tested whether WT sTREM2 could prevent neuronal loss induced by oligomeric A β at a molar ratio of 1:100 (sTREM2:A β monomer equivalents) conditions under which sTREM2 could not feasibly bind all the A β oligomers and found that WT sTREM2 still prevented the neuronal loss (Fig. S14), consistent with sTREM2 protecting by disaggregating A β oligomers. Overall, our results indicate that wild-type sTREM2 reduces A β neurotoxicity, while R47H TREM2 reduces the direct A β neurotoxicity less than WT sTREM2 and increases the A β neurotoxicity in cultures where microglia are present.

Discussion

We have shown that A β oligomers, but not A β monomers or fibrils, bind to microglial TREM2 and induce sTREM2 release, and this released sTREM2 also preferentially binds to A β oligomers, consistent with previous reports (13–15), (although Lessard *et al.* (15) did not find sTREM2 release in response to A β oligomers). Crucially, however, we also found that wild-type sTREM2 inhibits the formation of fibrils and larger A β oligomers and disaggregates protofibrils and larger A β oligomers into the smallest A β oligomers. This is consistent with a recent, preliminary report (30) that WT sTREM2 inhibited A β aggregation, measured by thioflavin T assay. In contrast, we found that R47H sTREM2 promoted the formation of A β protofibrils, indicating a gain of function by this mutation. These effects may provide a partial explanation of how a single copy of the TREM2 R47H mutant is associated

with increased risk for AD, by increasing production of neurotoxic forms of A β .

One potential caveat is the protein concentrations used in our experiments. In order to observe A β aggregation over a reasonable experimental timeframe, the lowest concentration of A β used here was 100 nM, whereas levels found in CSF are about 0.1 nM (10, 20, 31). However, the A β oligomer concentration near amyloid plaques was estimated as 700 nM (32), and plaques are likely to be a more relevant location for A β aggregation in AD than CSF. sTREM2 concentrations in lumbar CSF average about 0.2 nM (10, 20, 31); however again, it is likely that sTREM2 levels are higher near amyloid plaques surrounded by activated microglia, which express high levels of TREM2 (3). Note also that the observed effects of sTREM2 on A β are rapid: 20 nM sTREM2 dissolved 100 nM A β oligomers within 30 min *in vitro* (Fig. S11). Lower concentrations are likely to have the same disaggregating effect over a slower time course, which may be more relevant to the slow time course of AD.

We did not investigate the molecular mechanisms by which sTREM2 affected A β aggregation, but our finding that wildtype sTREM2 stabilizes the smallest observable oligomers (Figs. S9 and S11) suggests the possibility that sTREM2 binds preferentially to these (or undetectable oligomers such as dimers), thereby potentially blocking further growth of aggregates and disaggregating larger A β aggregates into smaller, potentially nontoxic forms. Precedent for this is the finding that α -synuclein-specific single-domain antibodies (nanobodies) bind α -synuclein stable oligomers and convert them into less stable oligomers with reduced toxicity (33). However, clearly more research is required to determine the mechanisms for sTREM2 and A β .

sTREM2 blocks A β aggregation and neurotoxicity

In summary, our experimental data reveal how A β oligomer binding to TREM2 may mediate direct (*via* activation of intracellular TREM2-dependent signaling pathways) and indirect protective mechanisms (*via* effects on A β oligomer assembly and toxicity). Our studies are broadly congruent with previous research showing that knockout of TREM2 expression in APP mice resulted in accelerated amyloid plaque seeding (17), with increased protofibrillar halos and hotspots around these plaques (3, 16, 18). Discrepant results were published for R47H TREM2 knockin mice (34), but these mice have been found to have little or no R47H TREM2 expression (35). However, these authors did show that WT sTREM2 bound strongly to amyloid plaques (34), consistent with our results. Our studies provide a potential explanation of the clinical observation of slower rates of cognitive and clinical decline in patients with MCI or AD who have higher levels of sTREM2 in the CSF (20, 21) and slower rates of amyloid deposition in healthy controls and MCI patients with higher sTREM2 levels in CSF (22). They also provide a potential explanation for the beneficial effects of infusing or expressing sTREM2 into the brain of mouse models of AD (16). Additional biophysical studies will be required to identify the key A β species dynamically interacting with wild-type sTREM2 to prevent neurotoxicity, and the A β species stabilized by sTREM2 R47H to increase neurotoxicity. This knowledge could be exploited for the design of small brain-penetrant molecular mimics of sTREM2 as potential therapeutics for AD.

Experimental procedures

cDNA constructs

Wild-type human TREM2 (hTREM2) and DAP12 (hDAP12) were subcloned in pCMV6-A vector (Origene). A single C \rightarrow A nucleotide polymorphism (SNP) at codon 85 (T85K) on the Origene TREM2 cDNA clone was reverted to consensus wild-type sequence by site-directed mutagenesis.

Antibodies

The following antibodies were used: mouse TREM2 (#AF1729, targeting on N-terminal TREM2, 1:500 for western blot; R&D); DDK (FLAG) (#TA50011, 1:2000 for western blot; Origene); V5 (#46-0705, 1:2000 for western blot; Life Technologies, Burlington); Nicastrin (#sc-14369, 1:200 for western blot; Santa Cruz); GAPDH (#2118, 1:3000 for western blot;

and anti-sheep IgG, 1:1000 for western blot after immunoprecipitation; Rockland); secondary antibodies conjugated with horseradish peroxidase (anti-mouse IgG; anti-rabbit IgG, 1:2000 for western blot; Thermo Scientific). Function-blocking TREM2 antibody (Clone 78.18, 25 μ g/ml for blocking assay, AbD Serotec catalogue number MCA4772EL) and a control antibody (Rat IgG1, AbD Serotec) were used for blocking experiments.

Animals

All experiments were performed in accordance with Canadian Council on Animal Care guidelines and UK Animals (Scientific Procedures) Act (1986) and approved by the Animal Care Committee at the University of Toronto and the Cambridge University local ethics committee.

TREM2-deficient mice were obtained from Dr J. Gommerman and were constructed by targeted homologous recombination (36), which removed Exon 1 and 2, which include the start codon and the major extracellular IgG domain. In contrast to the recently reported VelociGene construct, the direction of the Hygromycin cassette was “reversed.” Crucially, in agreement with two other models, but in contrast to the VelociGene construct, RT-PCR analyses confirmed specific loss of TREM2 expression without the perturbation of TREM1L expression observed in the VelociGene construct (36).

CRISPR-Cas 9 genome editing was used to create mouse models with mutations in Trem2 (R47H) at the Toronto Centre for Phenogenomics (37). Guide RNAs for each of the CRISPR genomic edits were assessed by two different programs for off-target sites (38, 39). Repair templates were designed to result in the desired amino acid substitution and to optimize or maintain comparable codon usage. The Trem2 R47H lines were validated by whole gene sequencing, RT-PCR, and western blotting. After breeding with C57BL/6 mice, heterozygous R47H/+ mice were then used to generate homozygous lines from each of the two founders. All genotyping was performed by genomic DNA sequencing. As with other similar CRISPR-Cas9 engineered mouse lines, this construct results in altered splicing and reduced expression (35), and consequently, we have not focused on the cell biology of the R47H microglia.

Gene edit	Guide RNA and location (Chr and strand)	Repair template	Primers
Trem2 R47H	gRNA-3 ACTGGGGGAGACGCAAGGCC Chr17:48548344 (+1)	CTGCAGGGCATGGCCGGCCA GTCCTTGAGGGTGTCTATGT ACTTATGACGCCCTGAAGC ACTGGGGGAGACaCAAGGC CTGGTGTCCGACGCTGGGTGA GGAGGGCCCATGCCAGCGT GTGGTGAGCACACAGGT GTGTGGCTGC	Trem2 PCR_F: GTGGAAGGTACC CAAGGACC Trem2 PCR_R: CAGGCACCTACAAGTAG CCC Trem2 Seq_F: TCTCCTCTGCAGC CCTGTC Trem 2 Seq_R: AGTACTGTGTA CTCACCTC.

Cell Signaling); Anti-His (C-term)-HRP (#46-0707, 1:2000 for dot blot, Invitrogen); A β (6E10, 1:1000 for western blot and dot blot, Covance); TrueBlot secondary antibodies conjugated with horseradish peroxidase (anti-goat IgG, anti-mouse IgG,

Primary microglial cell culture

Primary cultures of mixed glial cells and pure microglia were prepared from the cerebral cortex of P0-3-day-old C57BL/6 TREM2^{+/+} or TREM2^{-/-} mice as described (40).

sTREM2 blocks A β aggregation and neurotoxicity

After removal of olfactory bulbs, cerebral hemispheres were cut into ~ 1 mm pieces, vortexed for 1 min, filtered through a 40 μ m cell strainer, and plated in 80 cm² tissue culture flasks. Mixed glia were cultured until microglia appeared (10–18 days after plating). Microglia were isolated by shaking flasks. Purified microglia were replated for analysis. On average, each experiment used microglia from 30 to 35 pups. All pups used in this study (wild type; R47H, and TREM2KO) were maintained on a C57BL/6 background.

Mixed neuronal–glial cocultures and treatments

Mixed neuronal–glial cocultures were prepared from cerebella of 5–7-day-old rats (40), cultured for 7 days, then treated with either: vehicle, 250 nM monomeric amyloid beta 1–42 (A β), 250 nM A β + 25 nM wild-type sTREM2, or 250 nM A β + 25 nM R47H sTREM2 for 3 days. Three days later, neuronal death and loss were quantified by staining the live cultures with propidium iodide for necrosis, with isolectin IB4 for microglia, and with Hoechst 33342 for nuclei, which is used to distinguish healthy (uncondensed) from apoptotic (condensed) nuclei and to distinguish astrocytes (large bean-shaped nuclei) from neurons and microglia (small, round nuclei). Neurons are easily distinguished from astrocytes (by morphology) and from microglia (IB4 only binds microglia in these cultures), and the apoptotic neurons undergo strong nuclear condensation identified using the Hoechst 33342 staining (29, 40). The number of apoptotic, necrotic, and healthy neurons, astrocytes, and microglia are then counted on photos of multiple set fields, as previously described (29, 40). These cultures are 85 \pm 5% neurons, 7 \pm 3% astrocytes, and 5 \pm 3% microglia.

Amyloid β -peptide

Human A β 42 (used in TREM2 cleavage), HiLyte Fluor 488-labeled A β 42 (used in single-molecule TIRF imaging), HiLyte Fluor 647-labeled A β 42 (used in IP and dot blot), and Biotin-A β 42 (used in BLI) were purchased from AnaSpec and Bachem; A β 42 oligomers were prepared as endotoxin-free preparations (41) and validated by antibodies, gels, and electron microscopy (Fig. S1i). Prior work has established that these fluorescent tags do not significantly impact A β assembly (42).

Recombinant sTREM2 expression and purification

cDNAs encoding residues 19–143 of WT and R47H TREM2 were ordered as linear DNA strings (Life Technologies) and inserted into pHLSec. The plasmids were transfected into Freestyle 293-F cells (Life Technologies) grown in suspension in FreeStyle293 medium. Cells were transfected at a density of 2.5 \times 10⁶/ml with a DNA concentration of 3 μ g/ml and polyethyleneimine (Linear PEI 25 kDa molecular weight, Polysciences Inc) at 9 μ g/ml. On day 6 posttransfection, conditioned medium was harvested and TREM2 protein was purified using IMAC (Histrap excel, GE Healthcare) followed by gel filtration chromatography in storage buffer—20 mM HEPES, 200 mM NaCl, pH 7.0. The purity of WT and R47H sTREM2 was assessed by SDS-PAGE gels stained with Coomassie, which revealed only a single band for each (Fig. S15). To maintain a low

endotoxin level: endotoxin-free chemicals and plasticware were used; all chromatography media, columns, and concentrators (Vivaspin Turbo) were soaked for >12 h in 1 M NaOH. Proteins in storage buffer were concentrated to between 5 and 10 mg/ml for use and tested for endotoxin with the EndoZyme recombinant Factor C assay (Hyglos GmbH). Endotoxin levels in all assays were maintained at < 0.1 EU/ml.

Co-immunoprecipitation and western blot

Primary microglia were rinsed with ice-cold Dulbecco's modified Eagle medium without phenol red and incubated with 100 nM HiLyte Fluor 647-labeled A β at 4 $^{\circ}$ C for 1 h. For antibody blocking assays, before A β incubation, microglia cultures were preincubated with 25 μ g/ml monoclonal anti-TREM2 antibody or rat IgG1 control for 20 min. Cells were collected by scraping, washed with ice cold 1xPBS, and centrifuged. Primary microglia were lysed with 1% CHAPSO buffer (1% 3-[(3-cholamidopropyl) dimethylammonio]-2-hydroxy-1-propanesulfonate (CHAPSO), 25 mM HEPES, 150 mM NaCl, 2 mM EDTA, pH 7.4). Crude membrane fractions were extracted from HeLa cell pellets as described (43) and lysed with 1% CHAPSO buffer. Primary antibodies and corresponding IgG controls (1 μ g/reaction) were incubated with lysates at 4 $^{\circ}$ C for 2 h, then mixed with Protein G Dynabeads (Life Technologies), incubated at 23 $^{\circ}$ C for 20 min, then washed and eluted as per manufacturer's instructions. The immunoprecipitates were separated on 4–12% MES/Bis-Tris gels (Life Technologies). Fluorescent signals of A β were detected using an Odyssey FC imaging system (LI-COR). Proteins were transferred onto nitrocellulose membranes, which were probed with primary antibodies and corresponding TrueBlot secondary antibodies.

In vitro coprecipitation of TREM2 or TREM1 with A β oligomers was performed by mixing recombinant Fc-tagged TREM2 or TREM1 ectodomain (residues 19–171; 100 ng/ml, R&D systems), 100 nM HiLyte Fluor 647-labeled A β oligomers, and Protein G Dynabeads in 0.5% fatty acid free BSA PBS-Tween buffer. The mixture was incubated at room temperature for 1 h and then washed, eluted, and analyzed the same as described above.

Dot blot

A β monomers or oligomers (1 μ g/dot) prepared as described above and anti-TREM2 antibody (0.3 μ g/dot) were spotted onto a nitrocellulose membrane. Membrane strips were blocked with 3% fatty acid free BSA (Sigma Aldrich) and then incubated with 100 nM recombinant His-tagged WT/R47H TREM2 ECD diluted in blocking buffer at 4 $^{\circ}$ C for 1 h. Bound TREM2 ECDs were probed with HRP-conjugated anti-His tag antibody and detected with Odyssey FC imaging system.

Bio-layer interferometry

Preparation of A β oligomers for Bio-Layer Interferometry (BLI) studies

Synthetic human A β residues 1–42 and biotinylated A β 42 were purchased from Bachem or AnaSpec and solubilized in

hexafluoroisopropanol (HFIP) with DMSO (200 μ l) to generate monomeric species. Solubilized A β was diluted in filtered assay buffer (20 mM HEPES, 500 mM NaCl pH 7.4) containing DMSO (2%) to a total volume of 9800 μ l and a peptide concentration of 0.1 mg/ml (22 μ M). Peptide solutions were aliquoted and incubated for 3 h at 37 °C with stock solutions stored at -80 °C. TEM was performed using undiluted biotinylated A β (100%) or a mixture of biotinylated A β (10%) and unlabeled A β (90%), which were diluted to final concentrations of 1.1 μ M (Fig. S1, *iii* and *iv*). These TEM samples (10 μ l) were applied to carbonate coated grids and negatively stained with 1% phosphotungstic acid (PTA). TEM micrographs indicating the globular morphology of the A β oligomers were obtained on a Hitachi H-7000 operated at 75 kV. The biotinylated oligomers were indistinguishable from nonbiotinylated A β oligomers.

Binding affinity of TREM2 ectodomain to A β was analyzed by Bio-Layer Interferometry (BLI) using the Octet RED384 system (ForteBio)

Assays were performed at 30 °C in the assay buffer (20 mM HEPES, 500 mM NaCl, 0.1% w/v BSA, 0.02% v/v Tween20, pH 7.4) with vibration at 1000 rpm. Streptavidin biosensors loaded with Biotin-A β (Anaspec) were incubated with TREM2 ectodomain WT (1, 2, 5, 10 μ M) or R47H (2, 5, 10, 20 μ M) to obtain the association curves and subsequently in the assay buffer to obtain the dissociation curves. Kinetics data were analyzed using a 2:1 heterogeneous ligand model.

Single-molecule TIRF imaging

Aggregation of A β for TIRF studies

Stock solutions of HiLyte Fluor 488- labeled Human A β 42 (A β , 0.1 mg; AnaSpec) were prepared by dissolving the lyophilized peptide (1% NH₄OH, 50 μ l) followed by dilution into pH 7.4 PBS to 200 μ M, aliquoted, and stored at -80 °C. Working solutions were prepared by diluting the monomeric stock solutions into pH 7.4 PBS on ice to the concentration used for the aggregation (0.5 μ M). The working solution was then placed into a shaking incubator (3 °C, 200 rpm) for 6 h to ensure a significant population of oligomeric species. All protein samples were stored and diluted into LoBind microcentrifuge tubes (Eppendorf).

Preparation of slides for TIRF microscopy

Slides were prepared in the same way as previously described (23). Slides containing unlabeled A β and TREM2 were tested for fluorescence artefacts.

TIRF microscope setup

Colocalization experiments were performed on a bespoke TIRF setup. Continuous-wave solid-state lasers operating at 488 nm and 641 nm were used for imaging. The beam power was controlled by attenuation through a neutral density filter,

following which undesirable wavelengths were filtered out through excitation filters (LL01-488-25, FF01-640/14-25, Semrock). The beams were then circularly polarised by a quarter wave plate. Laser lines were combined by dichroic mirrors. The beams were then passed through a Köhler lens into the back aperture of an inverted microscope body (Olympus, IX73) and were reflected by a dichroic mirror (Di01-405/488/532/635, Semrock) through an oil immersion objective (Olympus, 60XOTIRF). Emitted radiation was collected through the same objective and passed through the dichroic before being filtered (FF01-480/40-25, LP02-647RU-25, Semrock). The fluorescence emission was then projected onto an EMCCD camera (Evolve Delta, Photometrics), each pixel was 275 nm in length. Data visualization was achieved through Micro-Manager and ImageJ software.

Single-molecule TIRF imaging

The colocalization experiment was designed to investigate binding of A β oligomers with TREM2. The A β 6 h aggregation contained a mixture of monomeric and oligomeric species, hence illumination was performed for significant time periods to photobleach the monomeric species. Automated TIRF colocalization experiments were performed with the use of a custom script (BeanShell, micromanager). Each data set consisted of a 3 \times 3 grid of nine images at different areas of the coverslide, distances between images was 350 μ m as previously described (20). Images were recorded at 33 ms exposure, beginning with 800 frames excitation with 641 nm followed by 800 frames excitation, 488 nm excitation in the same field of view.

Colocalization analysis

Colocalization data was analyzed with a bespoke ImageJ macro. The 488 nm illumination channel contained a mixture of monomeric and oligomeric A β species, it was determined that the majority of monomeric species were photobleached by 40 frames of 488 nm illumination. Therefore, only frames after this point were considered in this analysis. The 488 nm and 641 nm illumination channels were compressed in time to create two single-frame images representing the average pixel intensities. Following which, points of intensity representing HiLyte Fluor 488 A β or AF647-TREM2 above a background threshold were located, counted, and binary images of these maxima were created. The two images were then summed to identify colocalized points. Chance coincident spots were excluded by 90° rotation of the binary image representing AF647-TREM2 points and summation with the HiLyte Fluor 488 A β image. Chance coincident spots were subtracted from the actual coincidence value, and percentage coincidence was calculated with the equation below:

$$\text{Coincidence} = \left(\frac{N_{\text{A}\beta\text{-TREM2}}}{(N_{\text{A}\beta\text{-TREM2}} - N_{\text{A}\beta})} \right) \times 100$$

sTREM2 blocks A β aggregation and neurotoxicity

TREM2 cleavage assays

HEK293 cell lines

HEK293 cells stably coexpressing HaloTag-WT hTREM2 and hDAP12 were grown on six-well plates for 48 h. Media were replaced by treatment media (1 ml of OptiMEM supplemented with 0.5% FBS) containing defined concentrations of freshly made A β 42 oligomers or crude neuronal membrane lipid extracts. Cells were collected 16 h after treatment, and amounts of CTF-TREM2 were assayed by western blotting. NTF release in conditioned media was detected by specific binding of the fluorescently labeled HaloTag ligand, HaloTag TMR direct. In total, 20 μ l of media was loaded on gel, and the NTF-related fluorescence was detected using the LI-COR Odyssey imager. Where indicated, HEK293 cells were transfected with human TREM2 tagged at the N-terminus or with R47H or WT human TREM2 (together with human DAP12), as previously described (8).

Primary microglia

Primary microglia from wild and TREM2 mutant mice were isolated from mixed glia culture by shaking and grown on 96-well plates for 24 h. Media were replaced by treatment media (1 ml of OptiMEM supplemented with 0.5% FBS) containing defined concentrations of freshly made A β oligomers. Cells were collected 24 h after treatment, and NTF release in conditioned media and TREM2 in cell lysate were detected by ELISA. TREM2 ELISA was performed on 96-well plates previously coated by TREM2 antibody (clone 78.18) and blocked with 0.5% BSA in 0.05% Tween20 in 1 \times PBS (PBST). Medium or cell lysate samples were added to precoated wells and incubated overnight at 4 $^{\circ}$ C. After washing with PBST, wells were incubated with TREM2 antibody (sheep anti-mouse TREM2, AF1729) diluted in blocking buffer for 2 h at room temperature. After secondary antibody (anti-sheep-HRP, 1:5000) incubation for 1 h at room temperature and washing, TMB chromogenic substrate was added to each well and developed at room temperature in dark for 20 min. The absorbance at 450 nm was read immediately after stop solution was added. TREM2 cleavage was represented by the ratio of relative values of sTREM2 in medium and total TREM2 in cell lysate, after subtracting the corresponding background values from TREM2 KO microglia in the same ELISA experiment.

sTREM2 effects on A β oligomers

Preparation of A β oligomers and A β fibrils and sTREM2 treatment

HFIP-treated human synthetic A β 42 was purchased from Bachem. A β solubilized by DMSO was diluted in PBS (pH 7.4) to a peptide concentration of 0.1 mg/ml (22 μ M). To study sTREM2 effects on assembly of A β oligomers, monomeric A β (22 μ M) solutions were incubated with or without WT sTREM2 or sTREM2 R47H (sTREM2: A β , 1:100 or 1:50) for 3 h at 37 $^{\circ}$ C. To study reversal of oligomerization, monomeric A β (22 μ M) solutions were incubated for 3 h at 37 $^{\circ}$ C to make oligomers, then diluted and mixed with WT sTREM or sTREM2 R47H (sTREM2: A β , 1:5 or 1:1) to a A β concentration of 2.2 μ M.

Then A β and sTREM2 mixture was incubated for 30 min at 37 $^{\circ}$ C. To study dissociation of fibrils, monomeric A β (110 μ M) solutions were incubated for 24 h at 37 $^{\circ}$ C with shaking (150 rpm), then diluted and mixed with WT or R47H sTREM2 (sTREM2: A β , 1:1) to a A β concentration of 2.2 μ M, then incubated for 30 min, 2 h, or 24 h at 37 $^{\circ}$ C. These peptide solutions were then used for TEM, dot blot, and HPLC-SEC experiments.

Transmission electron microscopy (TEM)

A β oligomers were prepared as described above. TEM was performed to characterize A β or mixtures of sTREM2 and A β , which were diluted to final A β concentrations of 1.1 μ M or 100 nM. These TEM samples (10 μ l) were applied to carbonate-coated grids for 1 min and negatively stained with 1% phosphotungstic acid (PTA) for 1 min. TEM micrographs were obtained on a Hitachi H-7000 operated at 120 kV.

Dot blots

A β oligomers were prepared as described above. A β and mixtures of sTREM2 and A β oligomers (1 μ g/dot) prepared as described above were spotted onto a nitrocellulose membrane. Membrane strips were blocked with 5% fatty acid free BSA (Sigma Aldrich) and then incubated with antioligomer-specific antibody (A11, ThermoFisher Scientific) or anti-amyloid β sequence-specific antibody (4G8, Millipore) for 1 h at RT and probed with HRP-conjugated anti-rabbit or mouse IgG antibodies and detected with ChemiDoc XRS+ imaging system (Bio-Rad).

HPLC-SEC

A β oligomers were prepared as described above. The size of prepared A β peptides was analyzed by SEC. Samples were run on a BioSep SEC-S 4000 (Phenomenex) column using a ProStar 210 HPLC (Varian) system with a ProStar 325 UV detector (Varian). Injected samples were eluted with PBS (pH 7.4) at a flow rate of 0.5 ml/min at ambient temperature, and data were obtained at 280 nm. Peak areas were integrated using Star 6.2 Chromatography Workstation (Varian).

A β fibrillization assay

In total, 10 μ M of monomeric A β was incubated at 30 $^{\circ}$ C in DMEM/F12 with 10 μ M Thioflavin T \pm 1 μ M wild-type or R47H sTREM2 in Corning 96 Well White Polystyrene Microplate with a clear flat bottom in a FluoroSTAR Optima plate reader (with orbital shaking between readings) to monitor fluorescence. Alternatively, 2 μ M of monomeric A β was incubated at 37 $^{\circ}$ C in 20 mM phosphate buffer (pH 8) with 10 μ M Thioflavin T \pm 0, 0.02, 0.2, or 1.0 μ M wild-type or R47H sTREM2 in a fluorescence plate reader with a 440-nm excitation filter and a 480-nm emission filter without stirring as previously described (44).

Membrane permeabilization assay

Lipid vesicles were prepared as previously described (45), using a 100:1 mixture of phospholipids 16:0–18:1

phosphatidylcholine and biotinylated lipids 18:1–12:0 Biotin phosphatidylcholine. The mean diameter of vesicles was \sim 200 nm, and these were filled with 100 μ M Cal-520 dye using five freeze-and-thaw cycles. Nonincorporated Cal-520 dye was separated from the dye-filled vesicles by SEC. The vesicles were immobilized in biotin-labeled PLL-g-PEG-coated glass coverslips using a biotin–neutravidin linkage. Then coverslips were incubated with 50 μ l Ca $^{2+}$ containing buffer solution and different position of the coverslips imaged (F_{blank}). Stage movements were controlled using an automated bean BeanShell-based program, which allows fields-of-view selection without user bias. Then the 10 μ M aggregation (6-h time point) solution was added to the coverslips so that the final concentration of the peptide under the coverslip was 200 nM. Then the sample was incubated with the vesicles for 20 min, and the same fields of view of each coverslip were imaged (F_{sample}). Then, 10 μ l of 1 mg/ml of ionomycin was added to the same coverslips, and the same fields of view were imaged again ($F_{\text{ionomycin}}$). Ionomycin is a calcium ionophore and causes saturation of the fluorescence intensity observed. This allows us to normalize fluorescence originating from individual vesicles and subsequently quantify the sample-induced Ca $^{2+}$ influx using the following equation:

$$\text{Average Ca}^{2+} \text{ influx} = (F_{\text{sample}} - F_{\text{blank}}) / (F_{\text{ionomycin}} - F_{\text{blank}})$$

All the imaging was done using a Total Internal Reflection Fluorescence Microscope (TIRFM) based on an inverted Nikon Ti microscope. For excitation, a 488 nm laser beam was focused in the back focal plane of the 60 \times , 1.49 NA oil-immersion objective lens. Fluorescence signal emerged from the samples collected from the same objective and imaged by air-cooled EMCCD camera. All the imaging experiments were performed at 293K. Fluorescence images were acquired using a 488 nm laser (\sim 10 W/cm 2) for 50 frames with a scan speed of 20 Hz and analyzed using ImageJ to calculate the localized fluorescence intensity of each vesicle.

Statistics

All statistical analyses were performed using Prism (GraphPad Software Inc). Nonparametric statistical tests were used when data did not show a normal distribution. The specific statistical test used in each experiment is described in the associated figure legend. Data are expressed as means \pm SEM. Results were considered significant if $p < 0.05$. In most cases, the sample size (*i.e.*, the number of biological repeats, n) was 3, as indicated in the figure legends, and this number was selected as the default for experiments using isolated proteins, based on previous experience of variance sizes. In the case of Figure 3I, measuring the area of fibrils, the variance was found to be high (because the number of fibrils is low and size large), so n was increased to 8 for A β alone but remained at $n = 3$ for A β + WT or R47H sTREM2. For Figure 4D, which is a primary cell culture experiment, the sample size was 4, based on previous experience of variance sizes. The sample size n refers to biological

repeats, which means repeating using a different biological sample preparation. Outliers were only encountered in the data of Figure 2B and were identified and removed by using GraphPad Prism outlier calculator.

Data availability

The published article includes all data generated or analyzed during this study. Original source data for the figures in the paper are available upon request to the corresponding authors. No proprietary software was used in the data analysis. Further information and requests for resources and reagents should be directed to: gcb3@cam.ac.uk or phs22@cam.ac.uk

Supporting information—This article contains [supporting information](#).

Author contributions—A. V., Y. Z., J. S., J. K. G., K. S., D. H. A., S. D., M. P., A. B., M. A. B., R. B. D., F. C., Y. Z., S. Q., J. H., J. W., and P. E. F. performed and analyzed the molecular biological, biochemical, and cell biological experiments. K. S. and P. E. F. performed and analyzed assembly/disassembly assay. KS and PEF performed and analyzed electron microscopy experiments, SEC, and dot-blot assay. P. F. and D. K. performed and analyzed the permeabilization assay. L.-M. N., A. V., and S. F. L. performed and analyzed the single-molecule imaging experiments. K. S., M. E., and P. E. F. performed and analyzed the biophysical binding assay. P. S. G.-H. and G. C. B. conceived and directed the experiments and acquired funding. All the authors contributed to the writing of the article.

Funding and additional information—This project has received funding from the Canadian Institutes of Health Research (P. S. G.-H. and P. E. F.), Canadian Consortium on Neurodegeneration in Aging, Wellcome Trust, Medical Research Council, Zenith Award Alzheimer Association (P. S. G.-H.). This project has received funding from the Innovative Medicines Initiative 2 joint undertaking under grant agreement no. 115976. This joint undertaking receives support from the European Union's Horizon 2020 research and innovation program and European Federation of Pharmaceutical Industries and Associations (G. C. B., J. W., and P. S. G.-H.).

Conflict of interest—The authors declare that they have no conflicts of interest with the contents of this article.

Abbreviations—The abbreviations used are: AD, Alzheimer's disease; BLI, bio-layer interferometry; CSF, cerebrospinal fluid; CTF, C-terminal fragment; HPLC-SEC, high-performance liquid chromatography size-exclusion chromatography; MCI, mild cognitive impairment; TEM, transmission electron microscopy; TIRF, total internal reflection fluorescence; TREM2, triggering receptor expressed on myeloid cells 2.

References

1. Wong, C. W., Quaranta, V., and Glenner, G. G. (1985) Neuritic plaques and cerebrovascular amyloid in Alzheimer disease are antigenically related. *Proc. Natl. Acad. Sci. U. S. A.* **82**, 8729–8732
2. Edwards, F. A. (2019) A unifying hypothesis for Alzheimer's disease: From plaques to neurodegeneration. *Trends Neurosci.* **42**, 310–322
3. Yuan, P., Condello, C., Keene, C. D., Wang, Y., Bird, T. D., Paul, S. M., Luo, W., Colonna, M., Baddeley, D., and Grutzendler, J. (2016) TREM2

sTREM2 blocks A β aggregation and neurotoxicity

- haploinsufficiency in mice and humans impairs the microglia barrier function leading to decreased amyloid compaction and severe axonal dystrophy. *Neuron* **90**, 724–739
- Guerreiro, R., Wojtas, A., Bras, J., Carrasquillo, M., Rogava, E., Majounie, E., Cruchaga, C., Sassi, C., Kauwe, J. S., Younkin, S., Hazrati, L., Collinge, J., Pocock, J., Lashley, T., Williams, J., *et al.* (2013) TREM2 variants in Alzheimer's disease. *N. Engl. J. Med.* **368**, 117–127
 - Jonsson, T., Stefansson, H., Steinberg, S., Jonsson, J., Jonsson, P. V., Naedal, J., Bjornsson, S., Huttenlocher, J., Levey, A. I., Lah, J. J., Rujescu, D., Hampel, H., Giegling, I., Andreassen, O. A., Engedal, K., *et al.* (2013) Variant of TREM2 associated with the risk of Alzheimer's disease. *N. Engl. J. Med.* **368**, 107–116
 - Sims, R., van der Lee, S. J., Naj, A. C., Bellenguez, C., Badarinarayan, N., Jakobsdottir, J., Kunkle, B. W., Boland, A., Raybould, R., Bis, J. C., Martin, E. R., Grenier-Boley, B., Heilmann-Heimbach, S., Chouraki, V., Kuzma, A. B., *et al.* (2017) Rare coding variants in PLCG2, ABI3, and TREM2 implicate microglial-mediated innate immunity in Alzheimer's disease. *Nat. Genet.* **49**, 1373–1384
 - Wunderlich, P., Glebov, K., Kemmerling, N., Tien, N. T., Neumann, H., and Walter, J. (2013) Sequential proteolytic processing of the triggering receptor expressed on myeloid cells-2 (TREM2) protein by ectodomain shedding and γ -secretase-dependent intramembranous cleavage. *J. Biol. Chem.* **288**, 33027–33036
 - Thornton, P., Sevalle, J., Deery, M. J., Fraser, G., Zhou, Y., Ståhl, S., Franssen, E. H., Dodd, R. B., Qamar, S., Gomez Perez-Nievas, B., Nicol, L. S., Eketjäll, S., Revell, J., Jones, C., Billinton, A., *et al.* (2017) TREM2 shedding by cleavage at the H157-S158 bond is accelerated for the Alzheimer's disease-associated H157Y variant. *EMBO Mol. Med.* **9**, 1366–1378
 - Schlepckow, K., Kleinberger, G., Fukumori, A., Feederle, R., Lichtenthaler, S. F., Steiner, H., and Haass, C. (2017) An Alzheimer-associated TREM2 variant occurs at the ADAM cleavage site and affects shedding and phagocytic function. *EMBO Mol. Med.* **9**, 1356–1365
 - Suárez-Calvet, M., Morenas-Rodríguez, E., Kleinberger, G., Schlepckow, K., Araque Caballero, M.Á., Franzmeier, N., Capell, A., Fellerer, K., Nuscher, B., Eren, E., Levin, J., Deming, Y., Piccio, L., Karch, C. M., Cruchaga, C., *et al.* (2019) Early increase of CSF sTREM2 in Alzheimer's disease is associated with tau related-neurodegeneration but not with amyloid- β pathology. *Mol. Neurodegener.* **14**, 1
 - Suarez-Calvet, M., Araque Caballero, M.Á., Kleinberger, G., Bateman, R. J., Fagan, A. M., Morris, J. C., Levin, J., Danek, A., Ewers, M., Haass, C., *et al.* (2016) Early changes in CSF sTREM2 in dominantly inherited Alzheimer's disease occur after amyloid deposition and neuronal injury. *Sci. Transl. Med.* **8**, 369ra178
 - Suárez-Calvet, M., Kleinberger, G., Araque Caballero, M.Á., Brendel, M., Rominger, A., Alcolea, D., Fortea, J., Lleó, A., Blesa, R., Gispert, J. D., Sánchez-Valle, R., Antonell, A., Rami, L., Molinuevo, J. L., Brosseron, F., *et al.* (2016) sTREM2 cerebrospinal fluid levels are a potential biomarker for microglia activity in early-stage Alzheimer's disease and associate with neuronal injury markers. *EMBO Mol. Med.* **8**, 466–476
 - Zhao, Y., Wu, X., Li, X., Jiang, L. L., Gui, X., Liu, Y., Sun, Y., Zhu, B., Piña-Crespo, J. C., Zhang, M., Zhang, N., Chen, X., Bu, G., An, Z., and Huang, T. Y. (2018) TREM2 is a receptor for beta-amyloid that mediates microglial function. *Neuron* **97**, 1023–1031
 - Zhong, L., Wang, Z., Wang, D., Wang, Z., Martens, Y. A., Wu, L., Xu, Y., Wang, K., Li, J., Huang, R., Can, D., Xu, H., Bu, G., and Chen, X. F. (2018) Amyloid-beta modulates microglial responses by binding to the triggering receptor expressed on myeloid cells 2 (TREM2). *Mol. Neurodegener.* **13**, 15
 - Lessard, C. B., Malnik, S. L., Zhou, Y., Ladd, T. B., Cruz, P. E., Ran, Y., Mahan, T. E., Chakrabaty, P., Holtzman, D. M., Ulrich, J. D., Colonna, M., and Golde, T. E. (2018) High-affinity interactions and signal transduction between A β oligomers and TREM2. *EMBO Mol. Med.* **10**, e9027
 - Zhong, L., Xu, Y., Zhuo, R., Wang, T., Wang, K., Huang, R., Wang, D., Gao, Y., Zhu, Y., Sheng, X., Chen, K., Wang, N., Zhu, L., Can, D., Marten, Y., *et al.* (2019) Soluble TREM2 ameliorates pathological phenotypes by modulating microglial functions in an Alzheimer's disease model. *Nat. Commun.* **10**, 1365
 - Parhizkar, S., Arzberger, T., Brendel, M., Kleinberger, G., Deussing, M., Focke, C., Nuscher, B., Xiong, M., Ghasemigharagou, A., Katzmarski, N., Krasemann, S., Lichtenthaler, S. F., Müller, S. A., Colombo, A., and Monosor, L. S. (2019) Loss of TREM2 function increases amyloid seeding but reduces plaque-associated ApoE. *Nat. Neurosci.* **22**, 191–204
 - Wang, Y., Ulland, T. K., Ulrich, J. D., Song, W., Tzaferis, J. A., Hole, J. T., Yuan, P., Mahan, T. E., Shi, Y., Gilfillan, S., Cella, M., Grutzendler, J., DeMattos, R. B., Cirrito, J. R., Holtzman, D. M., *et al.* (2016) TREM2-mediated early microglial response limits diffusion and toxicity of amyloid plaques. *J. Exp. Med.* **213**, 667–675
 - Ma, L. Z., Tan, L., Bi, Y. L., Shen, X. N., Xu, W., Ma, Y. H., Li, H. Q., Dong, Q., and Yu, J. T. (2020) Dynamic changes of CSF sTREM2 in preclinical Alzheimer's disease: The CABLE study. *Mol. Neurodegener.* **15**, 25
 - Ewers, M., Franzmeier, N., Suárez-Calvet, M., Morenas-Rodríguez, E., Caballero, M. A. A., Kleinberger, G., Piccio, L., Cruchaga, C., Deming, Y., Dichgans, M., Trojanowski, J. Q., Shaw, L. M., Weiner, M. W., and Haass, C. (2019) Increased soluble TREM2 in cerebrospinal fluid is associated with reduced cognitive and clinical decline in Alzheimer's disease. *Sci. Transl. Med.* **11**, 507
 - Franzmeier, N., Suárez-Calvet, M., Frontzkowski, L., Moore, A., Hohmann, T. J., Morenas-Rodríguez, E., Nuscher, B., Shaw, L., Trojanowski, J. Q., Dichgans, M., Kleinberger, G., Haass, C., and Ewers, M. (2020) Alzheimer's Disease Neuroimaging Initiative (ADNI), Higher CSF sTREM2 attenuates ApoE4-related risk for cognitive decline and neurodegeneration. *Mol. Neurodegener.* **15**, 57
 - Ewers, M., Biechele, G., Suárez-Calvet, M., Sacher, C., Blume, T., Morenas-Rodríguez, E., Deming, Y., Piccio, L., Cruchaga, C., Kleinberger, G., Shaw, L., Trojanowski, J. Q., Herms, J., Dichgans, M., Alzheimer's Disease Neuroimaging Initiative (ADNI), *et al.* (2020) Higher CSF sTREM2 and microglia activation are associated with slower rates of beta-amyloid accumulation. *EMBO Mol. Med.* **12**, e12308
 - Horrocks, M. H., Lee, S. F., Gandhi, S., Magdalinou, N. K., Chen, S. W., Devine, M. J., Tosatto, L., Kjaergaard, M., Beckwith, J. S., Zetterberg, H., Iljina, M., Cremades, N., Dobson, C. M., Wood, N. W., and Klennerman, D. (2016) Single-molecule imaging of individual amyloid protein aggregates in human biofluids. *ACS Chem. Neurosci* **7**, 399–406
 - Concepcion, J., Witte, K., Wartchow, C., Choo, S., Yao, D., Persson, H., Wei, J., Li, P., Heidecker, B., Ma, W., Varma, R., Zhao, L. S., Perillat, D., Carricato, G., Recknor, M., *et al.* (2009) Label-free detection of biomolecular interactions using Bio-Layer Interferometry for kinetic characterization. *Comb. High Throughput Screen* **12**, 791–800
 - Harper, J. D., Wong, S. S., Lieber, C. M., and Lansbury, P. T., Jr. (1999) Assembly of A beta amyloid protofibrils: An in vitro model for a possible early event in Alzheimer's disease. *Biochemistry* **38**, 8972–8980
 - Nichols, M. R., Moss, M. A., and Reed, D. K. (2005) Amyloid-beta protofibrils differ from amyloid-beta aggregates induced in dilute hexafluoroisopropanol in stability and morphology. *J. Biol. Chem.* **280**, 2471–2480
 - De, S., Whiten, D. R., Ruggeri, F. S., Hughes, C., Rodrigues, M., Sideris, D. I., Taylor, C. G., Aprile, F. A., Muyldermans, S., Knowles, T. P. J., Vendruscolo, M., Bryant, C., Blennow, K., Skoog, I., and Kern, S. (2019) Soluble aggregates present in cerebrospinal fluid change in size and mechanism of toxicity during Alzheimer's disease progression. *Acta Neuropathol. Commun.* **7**, 120
 - De, S., Wirthensohn, D. C., Flagmeier, P., Hughes, C., Aprile, F. A., Ruggeri, F. S., Whiten, D. R., Emin, D., Xia, Z., Varela, J. A., Sormanni, P., Kundel, F., Knowles, T. P. J., Dobson, C. M., Bryant, C., *et al.* (2019) Different soluble aggregates of A β 42 can give rise to cellular toxicity through different mechanisms. *Nat. Commun.* **10**, 1541
 - Neniskyte, U., Neher, J. J., and Brown, G. C. (2011) Neuronal death induced by nanomolar amyloid β is mediated by primary phagocytosis of neurons by microglia. *J. Biol. Chem.* **286**, 39904–39913
 - Kober, D. L., Alexander-Brett, J. M., Karch, C. M., Cruchaga, C., Colonna, M., Holtzman, M. J., and Brett, T. J. (2020) Functional insights from biophysical study of TREM2 interactions with apoE and A β 1-42. *Alzheimers Dement.* <https://doi.org/10.1002/alz.12194>

31. Piccio, L., Deming, Y., Del-Águila, J. L., Ghezzi, L., Holtzman, D. M., Fagan, A. M., Fenoglio, C., Galimberti, D., Borroni, B., and Cruchaga, C. (2016) Cerebrospinal fluid soluble TREM2 is higher in Alzheimer disease and associated with mutation status. *Acta Neuropathol.* **131**, 925–933
32. Yang, T., Xu, H., Walsh, D. M., and Selkoe, D. J. (2017) Large soluble oligomers of amyloid β -protein from Alzheimer brain are far less neuroactive than the smaller oligomers to which they dissociate. *J. Neurosci.* **35**, 152–163
33. Iljina, M., Hong, L., Horrocks, M. H., Ludtmann, M. H., Choi, M. L., Hughes, C. D., Ruggeri, F. S., Williams, T., Buell, A. K., Lee, J. E., Gandhi, S., Lee, S. F., Bryant, C. E., Vendruscolo, M., Knowles, T. P. J., *et al.* (2017) Nanobodies raised against monomeric α -synuclein inhibit fibril formation and destabilize toxic oligomeric species. *BMC Biol.* **15**, 57
34. Song, W. M., Joshita, S., Zhou, Y., Ulland, T. K., Gilfillan, S., and Colonna, M. (2018) Humanized TREM2 mice reveal microglia-intrinsic and -extrinsic effects of R47H polymorphism. *J. Exp. Med.* **215**, 745–760
35. Xiang, X., Piers, T. M., Wefers, B., Zhu, K., Mallach, A., Brunner, B., Kleinberger, G., Song, W., Colonna, M., Herms, J., Wurst, W., Pocock, J. M., and Haass, C. (2018) The Trem2 R47H Alzheimer's risk variant impairs splicing and reduces Trem2 mRNA and protein in mice but not in humans. *Mol. Neurodegener.* **13**, 49
36. Kang, S. S., Kurti, A., Baker, K. E., Liu, C. C., Colonna, M., Ulrich, J. D., Holtzman, D. M., Bu, G., and Fand ryer, J. D. (2018) Behavioral and transcriptomic analysis of Trem2-null mice: Not all knockout mice are created equal. *Hum. Mol. Genet.* **27**, 211–223
37. Gertsenstein, M., and Nutter, L. M. J. (2018) Engineering point mutant and epitope-tagged alleles in mice using Cas9 RNA-guided nuclease. *Curr. Protoc. Mouse Biol.* **8**, 28–53
38. Hsu, P. D., Scott, D. A., Weinstein, J. A., Ran, F. A., Konermann, S., Agarwala, V., Li, Y., Fine, E. J., Wu, X., Shalem, O., Cradick, T. J., Marraffini, L. A., Bao, G., and Zhang, F. (2013) DNA targeting specificity of RNA-guided Cas9 nucleases. *Nat. Biotechnol.* **31**, 827–832
39. Doench, J. G., Hartenian, E., Graham, D. B., Tothova, Z., Hegde, M., Smith, I., Sullender, M., Ebert, B. L., Xavier, R. J., and Root, D. E. (2014) Rational design of highly active sgRNAs for CRISPR-Cas9-mediated gene inactivation. *Nat. Biotechnol.* **32**, 1262–1267
40. Bal-Price, A., and Brown, G. C. (2001) Inflammatory neurodegeneration mediated by nitric oxide from activated glia-inhibiting neuronal respiration, causing glutamate release and excitotoxicity. *J. Neurosci.* **21**, 6480–6491
41. Stine, W. B., Jr., Dahlgren, K. N., Krafft, G. A., and LaDu, M. J. (2003) In vitro characterization of conditions for amyloid-beta peptide oligomerization and fibrillogenesis. *J. Biol. Chem.* **278**, 11612–11622
42. Drews, A., Flint, J., Shivji, N., Jönsson, P., Wirthensohn, D., De Genst, E., Vincke, C., Muyltermans, S., Dobson, C., and Klenerman, D. (2016) Individual aggregates of amyloid beta induce temporary calcium influx through the cell membrane of neuronal cells. *Sci. Rep.* **6**, 31910
43. Sevalle, J., Amoyel, A., Robert, P., Fournié-Zaluski, M. C., Roques, B., Checler, F., *et al.* (2009) Aminopeptidase A contributes to the N-terminal truncation of amyloid beta-peptide. *J. Neurochem.* **109**, 248–256
44. Chia, S., Flagmeier, P., Habchi, J., Lattanzi, V., Linse, S., Dobson, C. M., Knowles, T. P. J., and Vendruscolo, M. (2017) Monomeric and fibrillar α -synuclein exert opposite effects on the catalytic cycle that promotes the proliferation of A β 42 aggregates. *Proc. Natl. Acad. Sci. U. S. A.* **114**, 8005–8010
45. Flagmeier, P., De, S., Wirthensohn, D. C., Lee, S. F., Vincke, C., Muyltermans, S., Knowles, T. P. J., Gandhi, S., Dobson, C. M., and Klenerman, D. (2017) Ultrasensitive measurement of Ca²⁺ influx into lipid vesicles induced by protein aggregates. *Angew. Chem. Int. Ed* **56**, 7750–7754